INTERNATIONAL JOURNAL OF CONSERVATION SCIENCE

ISSN: 2067-533X Volume 17, Issue 3, 2026: 995-1010 www.ijcs.ro

DOI: 10. 36868/IJCS.2026.03.10

CHARACTERIZATION OF DECORATIVE ELEMENTS (*STUCCOES, MORTARS AND PLASTER LAYERS*) IN ALEXAN PASHA PALACE, ASSIUT, EGYPT

Abdel-Naser MAKLED[1], Amr OSMAN[1,2], Abdalla KAMEL[3], Mohamed EL-GOHARY[4*]

[1] Department of Conservation, Faculty of Archaeology, Sohag University, Sohag, Egypt
[2] Department of Archaeology, College of Tourism & Archaeology, King Saud University, KSA.
[3] Department of Conservation, Faculty of Archaeology, Cairo University, Giza, Egypt
[4] Department of Conservation, Faculty of Archaeology, Zagazug University, Zagazug, Egypt

Abstract

This paper is a contribution concerning the used building materials in Alexan Pasha Palace in Assiut that dates back to the 20th century. Since those building materials are exposed to damage over time, this paper focuses on an archaeometric analysis of selected original samples of some joining and decorative building materials (stucco layers, mortars, and plaster) to determine their composition in terms of raw materials and manufacturing technology. That helps in making the correct and suitable decision for the restoration plan. Samples underwent PLM, XRD, SEM-EDX, FTIR, and TGA/DTA analyses and investigations, revealing that calcite, gypsum, and quartz are the main components of raw materials used, in addition to some additives that were used for improving the mechanical properties and the aesthetic workability of main building materials. Severe deterioration conditions over a 120-year period resulted in a decayed microstructure of materials networks. Furthermore, the findings highlighted the crystal changes of the gypsum and calcite over time that were attributed to severe dominated conditions. In conclusion, these results will be used in the conservation-restoration interventions of the decoration elements that contribute to the continuity of the artistic and aesthetic value of the palace and such similar cases.

Keywords: *Decorative elements; Stucco; Plaster; Mortars; Conservation; Alexan Pasha Palace; Assiut*

Introduction

The research explores the historical importance of a grand palace associated with Alexan Pasha Absakharoun, a prominent figure who served in both the Parliament and the Senate during the late 19th century and the 1st half of the 20th century. Alexan Pasha hailed from distinguished Coptic families in the city of Assiut. *Alexan Pasha Palace* (Fig. 1) is located on Nile Street, south of the Assiut Governorate at coordinates 27°11'20"N 31°11'30"E. It is bordered on the eastern side by the Nile River. This palace dates back to the beginning of the 20th century (1910), as it is engraved on its main southern facade. The palace itself is an imposing structure situated within a sprawling garden covering approximately one and a half acres, enclosed by a protective wall on all sides; it stands as a testament to the past. Beyond its historical significance, the palace boasts a rich array of construction materials. Its walls, for instance, were meticulously crafted from red brick and limestone, while the roof features a sturdy framework of iron beams interwoven with bricks [1].

* Corresponding author: m_1968_algohary@yahoo.com

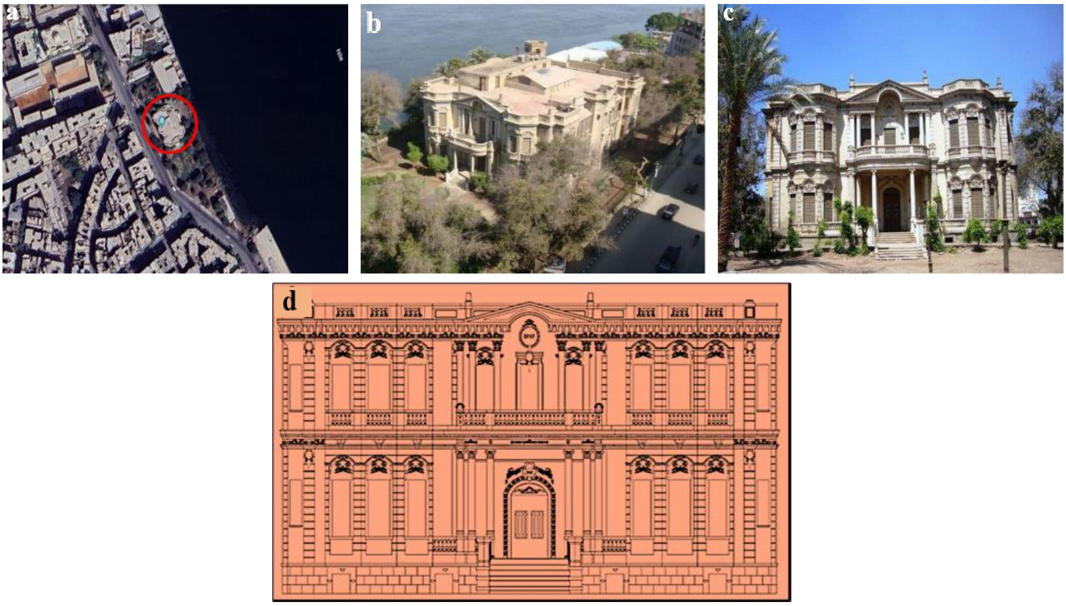

Fig .1. a. Satellite view of Alexan Pasha Palace; **b.** Bird's-eye view of the palace; **c.** The main southern façade of the palace; **d.** The elevation of the main southern façade

Notably, the palace's architectural distinction extends to its decorative elements. Elaborate stucco work, both colored and non-colored, adorns its surfaces. Additionally, the incorporation of colored glass drawings further enhances its aesthetic appeal. Given the unique blend of historical, artistic, and material values embodied by this structure, preservation becomes paramount. This palace holds significant historical importance within the context of its time, particularly among the other palaces scattered across Upper Egypt [2]. According to El-Gohary [3], field observation and some investigations were adapted through some scientific methods to evaluate the condition assessment of the palace. These methods include photographic recording and digital image processing (*PRDIP*), in addition to close inspection and complimentary survey (*CICS*) [4-7]. Through the resulting data of the previous investigations, it necessitates diligent attention, care, and maintenance to ensure its preservation. Over time, these delicate decorations and materials face the risk of deterioration. Safeguarding them ensures that future generations can appreciate and study this remarkable piece of history.

As asserted previously by El-Gohary [8], Pesaresi & Rizzi [9], Kamel et al. [10], and El-Gohary & Metawa [11], the preservation of architectural heritage and archaeological structures, with their unique façades and intricate decorative elements, plays a crucial role in safeguarding our human and civilizational legacy for future generations; one such remarkable site is the Alexan Pasha Palace in Assiut. Over time, this historical gem has faced various environmental hazards [12] that include *moisture*, *salt weathering*, *wind*, and *air pollution*, which have taken their toll. Additionally, *human-related factors* have contributed to its deterioration roles, as argued before by Nicu [13], Walsh et al. [14], and El-Gohary & Abdel Moneim [15]; in different cases, to ensure its longevity, restoration efforts are imperative. A comprehensive approach was employed, involving multiple tests and analyses for studying and examining some samples of these materials to ascertain their constituent elements and to facilitate a methodological study of their architectural and meticulous restoration. According to many specialists [16-19], the restoration process of stucco mortars was undertaken with dual objectives in mind. The primary objective was to fabricate benchmark stucco specimens that are congruent with the chemical and mineralogical composition of the original archaeological stucco [20].

The second objective was to develop a mortar tailored for the completion of stucco motifs, the application of pointing mortars, and the infilling of fissures [21], [22]. By analyzing historic building materials, the authors gain valuable insights into the building's evolution over time [23]. This knowledge informs restoration strategies, ensuring that the architectural legacy of Alexan Pasha Palace endures for generations to come. The present work relies on the study of the decorative building materials (*stuccoes*, *plaster,* and *mortars*) in Alexan Palace, aiming to develop a scientifically informed treatment plan. However, this process does not occur instantaneously; therefore, any research findings generated with the assistance of artificial intelligence must be rigorously verified and cross-referenced with traditionally established and reliable sources of knowledge [2]. Nonetheless, certain specific aspects of scientific research can benefit from AI support, potentially enhancing both experimental procedures and the reliability of obtained results. At its current level of advancement, artificial intelligence should be regarded as a supplementary research tool, applicable within clearly defined parameters [3]. Importantly, every scientific study represents an original and independent outcome of research efforts, rather than a mere AI-generated response. The experiment discussed in this article was conducted in accordance with this approach, utilizing AI in an indirect and controlled manner.

Materials and Methods

Materials

Initial visual examination has been carried out via in-situ visits according to El-Gohary [23] to identify the deterioration aspects [24]. Small representative samples of building materials have been carefully acquired and isolated from various building materials collected for examination and analyses to identify their chemical and mineralogical components. These components reflected the nature of the building materials and their physio-chemical properties, which is necessary when choosing and preparing the restoration materials for the archaeological site, including those samples: (**A**) *Internal layer of stucco sample*, (**B**) *External layer of stucco sample*, (**C**) *Jointing mortars sample*, and (**D**) *Plaster sample are* summarized in Table 1. Then, samples were captured and documented using a D5200 Canon digital camera.

Table 1. Description of the samples collected for the study

Symbol	Description	Features	Symbol	Description	Features
A	Internal layer of stucco		**B**	External layer of stucco	
C	Jointing mortars		**D**	Plaster	

Methods

Polarizing microscope (PLM)

The next step, samples, went under examination and analysis procedures by multidisciplinary sophisticated techniques to achieve a valuable characterization [25] as follows: Firstly, a thin section of each sample has been prepared by impregnating with low-viscosity epoxy resin under vacuum, and then they were sawn and polished until a thickness of 30 μm. Finally, the thin sections were meticulously analyzed using a polarizing microscope. This examination was instrumental in identifying the aggregates comprising various mineral additives (notably latent hydraulic components), the nature of the binder, and particles associated with the binder. Additionally, it provided a detailed description of the pore structure within the samples [26] to check the details of the type, condition, deterioration products, and hydraulic phases if present [27]. A *ZEISS polarizing microscope,* "Primptech," for transmitted and reflected light illumination with a built-in camera was used.

Mineralogical analysis (XRD)

The mineralogical analysis of the samples was performed by X-ray diffraction (XRD). *Brucker D8 Advance* has a theta: theta geometry (often called Bragg-Brentano or focusing geometry) with a copper-sealed tube x-ray source producing Cu Kα radiation (technically Kα1 and Kα2, with Kβ being removed by the primary optic) at a wavelength of 1.5406 Å from a generator operating at 40 kV and 40 mA. This machine operates using a copper line-focus X-ray tube producing Kα radiation (Kα1 = 1.540598 Å, Kα2 = 1.544426 Å, Kα ratio 0.5, Kαav = 1.541874 Å) at Sohag University.

Scanning electron microscopy with energy-dispersive X-ray spectroscopy (SEM-EDX)

Scanning electron microscopy with energy-dispersive X-ray spectroscopy (SEM-EDX) to study the morphology and chemical composition of the samples [28]. *SEM; FEI Quanta FEG 250 instruments*. The spectroscopic analysis of the energy-dispersive X-ray (EDX) was measured on an *SEM instrument (Quanta field emission gun (FEG) equipped with an Oxford EDX system)* at the Desert Research Center. Since it is one of the most important analyses that can be used as a helping tool in the reconstruction of historic stucco mortars [20].

Fourier-transform infrared spectroscopy (FTIR)

FTIR analysis was performed on the samples using *FTIR 460 Plus (Jasco, Japan)* in the range of 400-4000 cm^{-1} to identify their functional groups [29] at the microanalytical center at Cairo Univ.

Thermogravimetric analyzer and differential thermal analyzer (TGA/DTA)

According to Bader and Al-Gharib [30], *TGA/DTA* was conducted for the quantitative determination of calcium carbonate and dihydrate calcium sulfate, using a device with the following specifications: Detector: DTG-60H, Cell: platinum, Temp. rate: 10°C/min, Hold temp.: 1000°C.

Results

PLM

The results of the thin sections' examination are presented in Figure 2. Stucco samples exhibited calcite and fine-grained quartz grains, which appeared as sub-rounded to angular shapes. The jointing mortar sample also contains calcite and quartz within an iron-rich matrix, accompanied by iron oxides, gypsum, and fine-grained quartz. Lastly, PLM results confirm that lime is the main component in stucco and balding mortars. Finally, some cracks and surface discoloration surrounding the stucco were noted.

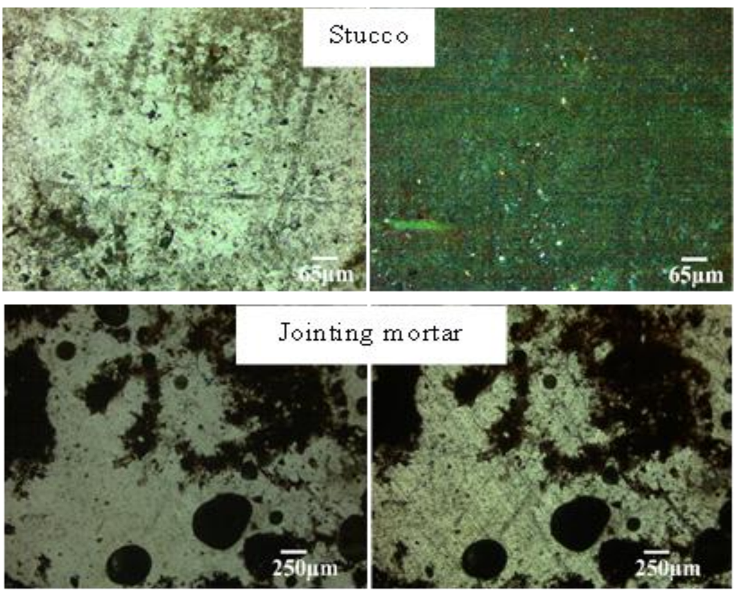

Fig. 2. Stucco and joining mortar samples under **a.** plane polarized (up) and **b.** cross polarized (down), respectively

XRD

The XRD results of samples taken from different places in Alexan Pasha Palace are listed in Table 2. The analysis of stucco samples' internal layer (A) decorative elements and the analysis of the mineralogical components, Figure 3a, revealed that it consisted of gypsum (89.5%), calcite (8.95%), and quartz (1.55); and the stucco samples' external layer (B) components, Figure 3b, included gypsum (34.2%), calcite (36.75%), quartz (13.05%), and dolomite (15.97%). Moreover, jointing mortar components (C). Figure 3c was calcite (11.45%), quartz (30%), dolomite (20.6%), hematite (23.2%), and magnetite (14.6%). Hematite and magnetite confirm the presence of iron compounds, which are responsible for the reddish-brown color of the mortar. Furthermore, the samples of plaster layer (D), Figure 3d, are composed essentially of gypsum (23.95%), calcite (59.3%), and quartz (16.75%), wherein gypsum was identified as the main component. Quartz was detected in all samples, and calcite, which was added to improve mechanical properties, was a major component in some samples of ancient plaster [31], [32].

Table 2. Average of XRD results of the examined samples: (A) stucco (internal layer), (B) stucco (external layer), (C) Jointing mortars, (D) plaster layer

Samples	Gyp	Cal	Qz	Dol	Hem	Mag_n	Mag_n. Cal
A	89.5	8.95	1.55	-	-	-	-
B	34.2	36.75	13.05	15.97	-	-	-
C	-	11.45	30	20.6	23.2	14.6	-
D	-	11.5	30	20.6	23.2	14.6	-

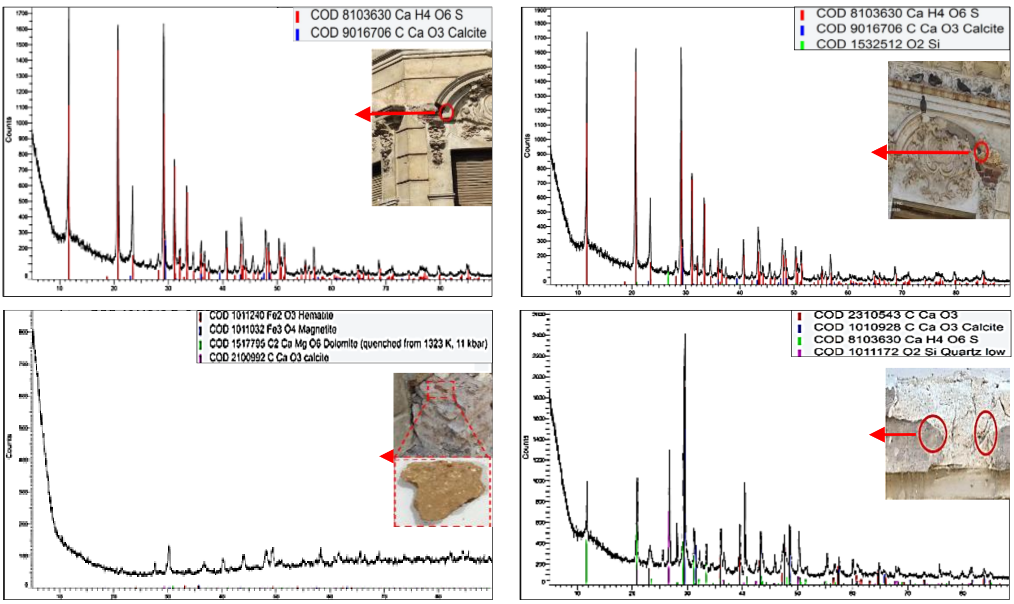

Fig. 3. XRD patterns of the examined samples; left - stucco (internal layer), right - stucco (external layer), Lower left - Jointing mortars, lower right - plaster layer

SEM

Scanning electron microscopy (SEM) microanalysis of samples from both the stucco internal and external layers revealed the fine platy calcite crystals supported by flax fibers, Figure 4a, in addition to prismatic needle-shaped gypsum crystals, Figure 4b. Further SEM investigation focused on the jointing mortar samples, indicating the use of lime mortar composed of calcite and angular to rounded quartz crystals, in addition to red brick crumbs characterized by grain homogeneity and slight porosity, and glassy phases suggested the utilization of high firing temperatures during brick manufacturing (Figure 4c). Within the same context, SEM investigation of the plaster sample, Figure 4d, attested that it was composed of a fine layer of platy calcite crystals and a fine-medium sand ratio.

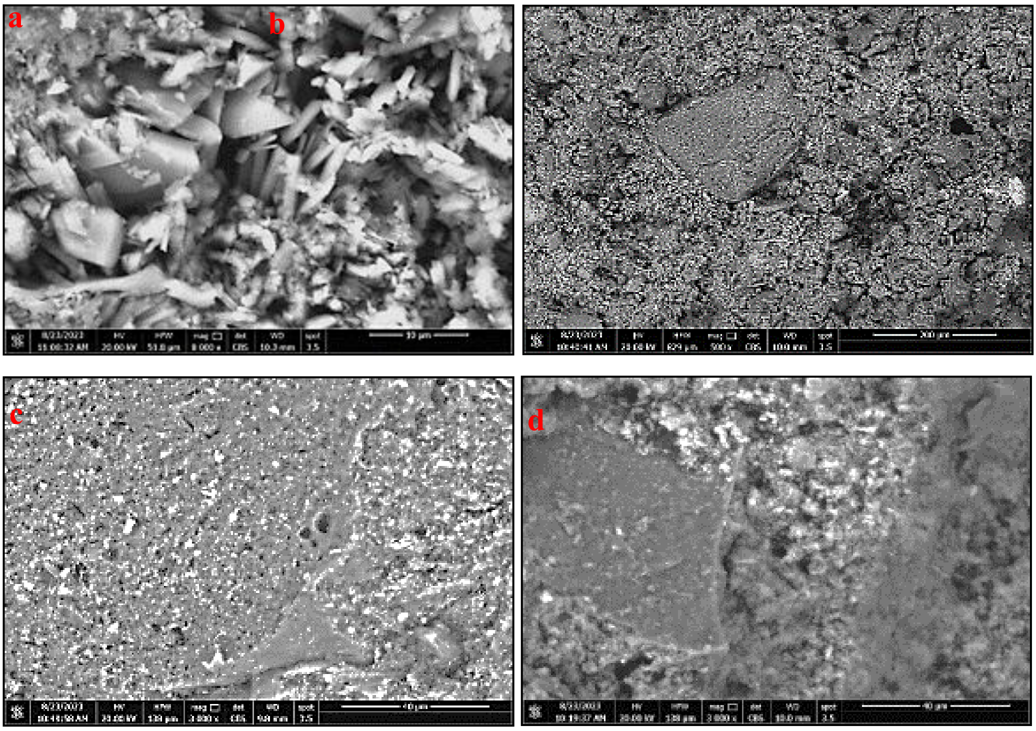

Fig. 4. SEM photomicrographs of the studied samples; **a.** stucco (internal layer), **b.** stucco (external layer), **c.** Jointing mortars, **d.** plaster

EDX

EDX microanalysis of samples listed in Table 3 proved that there are notable varieties of elements according to the type of the sample. The stucco internal and external layers, Figure 5a & b, revealed the presence of O, S, and Ca. These data demonstrated that gypsum ($CaSO_4.2H_2O$) was the predominant component in these samples. Additionally, varying percentages of Al, Si, Cl, Al, Na, Mg, K, and Fe were detected. Furthermore, the jointing mortar samples, Figure 5c, indicated a high concentration of Si, Ca, and C. Other elements such as Fe, Na, Mg, Al, S, and Cl were also detected in varying proportions. The increased calcium content confirmed the presence of calcite, likely added to enhance mechanical properties. Finally, the EDX microanalysis of the plaster sample, Figure 5d, highlighted major ions such as Si, Ca, and Cl along with minor elements like C, Na, Al, and K. These findings were corroborated by XRD and FTIR analyses.

Table 3. EDX atomic weight percentage analytical results of the stucco samples: (A) stucco (internal layer), (B) stucco samples (external layer), (C) samples Al-Aramis mortars, (D) plaster samples

	Elemental ratios %									
Samples	**C**	**O**	**Na**	**Mg**	**Al**	**Si**	**S**	**Cl**	**K**	**Ca**	**Fe**
A	2.7	47.4	0.4	--	0.3	0.3	17.8	2.1	0.4	28.6	--
B	15.4	37.7	0.2	0.2	0.5	0.8	15.4	1.3	0.3	27.6	0.6
C	4.0	42.1	1.1	0.9	2.3	11.1	0.4	6.5	0.8	28.8	2.1
D	3.5	38.1	0.4	--	0.8	2.8	--	5.5	0.4	48.6	--

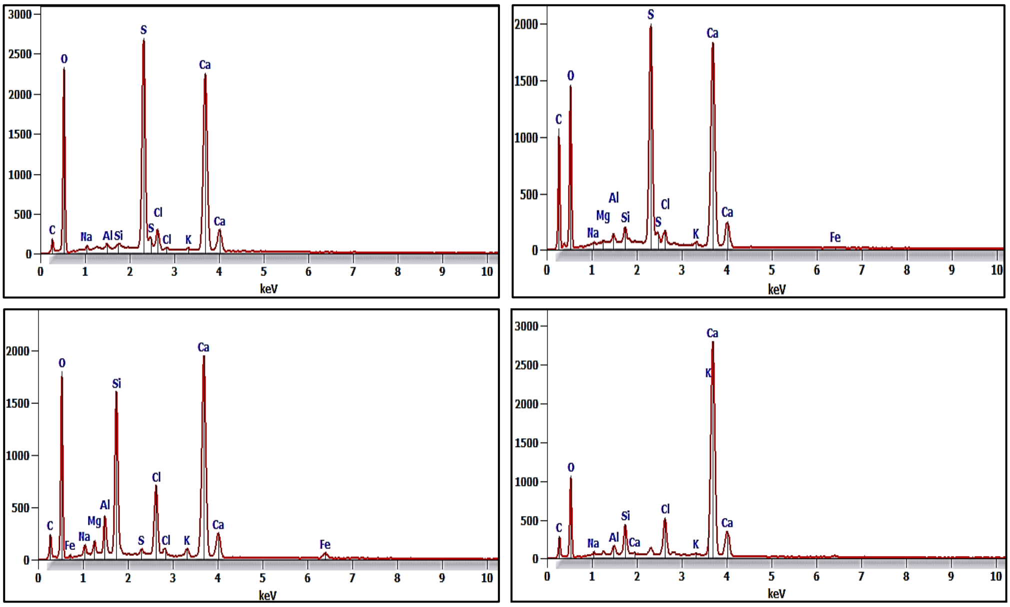

Fig. 5. EDX patterns of the studied samples; upper left - stucco (internal layer), upper right - stucco (external layer), lower left - Jointing mortars, lower right - plaster

FTIR

The Fourier-transform infrared (FTIR) results for stucco samples from both internal and external layers, Figure 6a & b, reveal distinctive absorption bands associated with gypsum. These bands correspond to stretching frequencies of O-H bonds (3547.41 cm^{-1}, 3548.38 cm^{-1}, 3406.64 cm^{-1}, and 3407.6 cm^{-1}) and a bond at 1467.56 cm^{-1}.

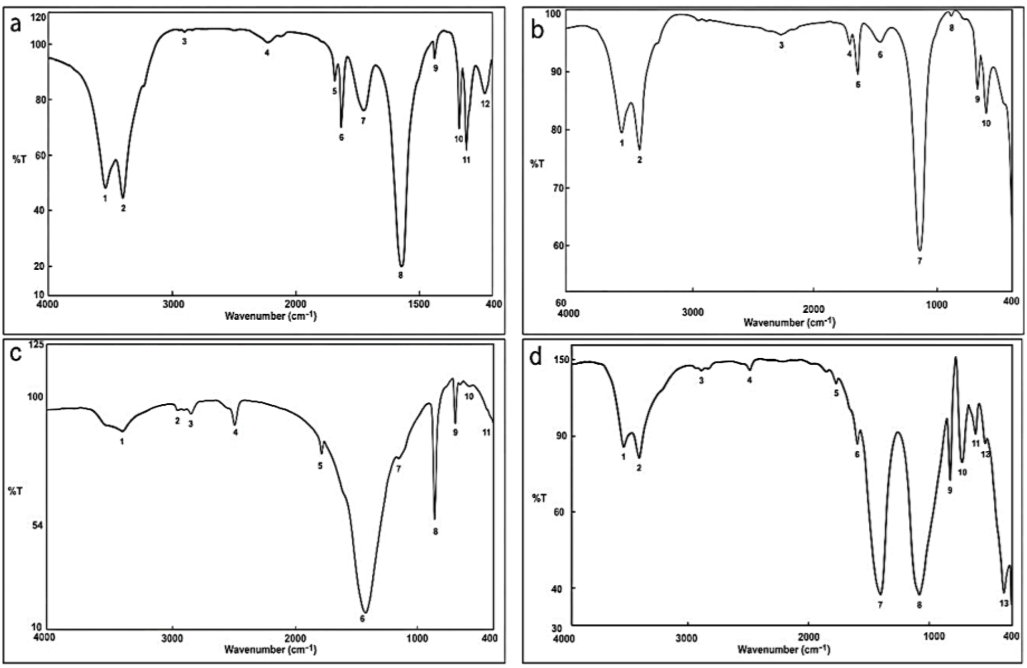

Fig. 6. Infrared spectra of samples; **a.** stucco (internal layer), **b.** stucco (external layer), **c.** Jointing mortars, **d.** plaster mortar

Additionally, calcium sulfate exhibits absorption bands at 670 cm⁻¹, while calcite manifests through stretching vibrations at 1623.77 cm⁻¹ and 1622.8 cm⁻¹, as well as a bond at 602.646 cm⁻¹. Similarly, jointing mortars, Figure 6c, exhibit gypsum identification through absorption bands associated with stretching vibrations. Calcium sulfate absorption is observed at 3426.89 cm⁻¹, calcite at 1629.55 cm⁻¹ and 876.488 cm⁻¹, and quartz at the stretching vibration bond of 1040.41 cm⁻¹. FTIR analysis confirms the presence of gypsum through absorption bands related to stretching vibrations. Furthermore, calcium sulfate absorption occurs at 3413.39 cm⁻¹, and calcite exhibits stretching vibrations at 709.676 cm⁻¹ and 874.56 cm⁻¹. Finally, the FTIR results for plaster layer samples, Figure 6d, highlight gypsum through absorption bands related to stretching vibrations of calcium sulfate at 3545.49 cm⁻¹ and 3407.6 cm⁻¹. Calcite is evident through stretching vibrations at 783.922 cm⁻¹ and 875.524 cm⁻¹, while quartz exhibits a stretching vibration bond at 1040.41 cm⁻¹ [33].

DTA/TGA

The results of thermal analysis revealed the following: Curves A and B, representing the *external layer of stucco* (Figure 7a & b), display a pronounced endothermic peak at ~149°C associated with gypsum dehydration [34], accompanied by a high mass-loss event of ~16.75% between 24 and 324°C, confirming a gypsum-rich matrix; a secondary peak at ~658°C and a corresponding 4.16% mass loss between 324 and 714°C indicate the presence of calcite [35], [36], though in lower proportion, suggesting a binder dominated by gypsum with minor carbonate inclusions. Curves C and D (*Stucco internal layer*), Figure 7c & d, similarly exhibit a sharp gypsum-dehydration peak at ~147°C and a DTG mass-loss event at ~143°C, reflecting high gypsum purity and good crystallinity, while the decomposition of calcite at ~653°C confirms a mixed but gypsum-dominant composition typical of protected internal layers with minimal alteration. In contrast, curves E and F (*Jointing mortar*), Figure 7e & f, show a markedly different thermal signature: the DTA peak at ~645°C and DTG mass loss at ~642°C indicate calcite decomposition as the principal thermal event, while the low-temperature peak at ~76°C reflects minor dehydration, collectively demonstrating a carbonate-rich, lime-based mortar with only limited or altered gypsum traces—consistent with its structural rather than finishing function. Curves G and H (*Plaster layer*), Figure 7g & h, present dual endothermic events at ~151°C and ~706°C corresponding to gypsum dehydration and calcite decomposition, respectively, with DTG data confirming both transitions; however, the relative intensity of the high-temperature peak suggests a more substantial carbonate component compared to samples 1 and 2, indicating a mixed gypsum–lime plaster formulation.

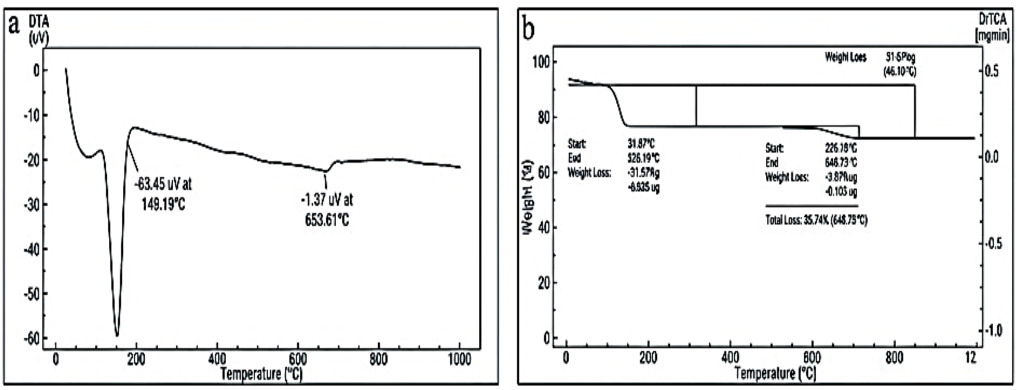

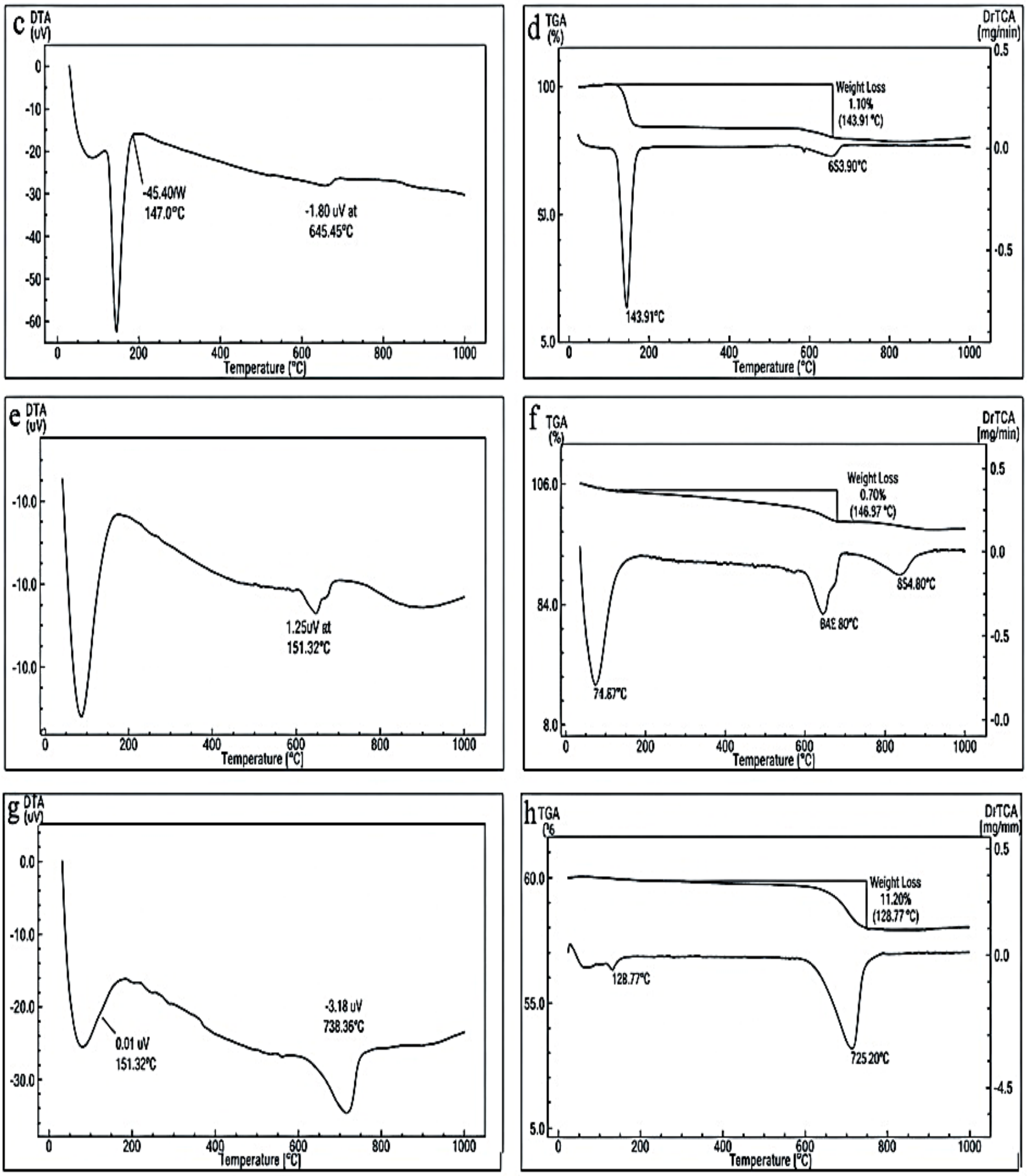

Fig. 7. TG-DTA curves of decorative elements; **a.** & **b.** stucco external layers, **c.** & **d.** stucco internal layers, **e.** & **f.** Jointing mortar, **g.** & **h.** plaster layers

Discussion

The completion of damaged or collapsed antiquities is among the most important and delicate operations in antiquity restoration and conservation. It contributes significantly to the stability and survival of historical buildings and decorations, preserving their artistic and architectural details and enabling them to maintain their original function. Furthermore, the completion of archaeological buildings and decorations, whether partial or full, aims to restore their original appearance and eliminate structural weaknesses in the buildings and in decorative elements and stucco. Within the same context, when completing decorative elements, inscriptions, or geometric shapes, it is essential to employ existing documents, references, or guides that provide evidence of the missing parts. Moreover, the original execution methods should be adopted, and the same metallic components used in the decorations should be identified through sample examinations and analyses.

In this regard, our findings proved that thin section analysis revealed some textural differences among the studied samples, in accordance with macroscopic observations, Figure 2. Overall, in mortars, stucco samples exhibited calcite and fine-grained quartz grains, which appeared as sub-rounded to angular shapes, indicating an origin from natural sands as reported before by El-Gohary [37] in a similar case. The presence of well-rounded porous lime lumps indicates that the lime used was dry-slaked, i.e., slaked with a minimum amount of water to convert all CaO into $Ca(OH)_2$ [26]. While it could be affirmed that the presence of iron minerals in the jointing mortar samples indicated the presence of red brick fragments in the mortar [38], [39]. Furthermore, minor crystals of calcite were observed within a notable pore with some brick fragments on the internal surface of the investigated samples, Figure 2a, as discussed previously by Uccelli [40]. Also, quartz as silicate impurities has been observed as an accessory mineral. Plagioclase and iron oxide fine aggregates can be noted as rounded and subangular components within the sample that could be attributed to some additives during the stucco preparation. Regarding the notable cracking and surface discoloration affected the case study owed accurately to the effect of humid environments and composition of rust that can be attacked very strongly by gypsum [41]. The studied samples, by XRD (Table 2 & Fig. 3), show that the *stucco* samples consist mainly of calcite ($CaCO_3$), gypsum ($CaSO_4 \cdot 2H_2O$), and dolomite ($(CaMg)CO_3$), in addition to a small amount of quartz (SiO_2).

These minerals that represent the main components characterized the historical stucco used in many historical palaces due to its versatility in creating intricate and durable decorative elements, as could be noted in *Baroque* and *Rococo* [42], [43], [44]. Within the same context, the presence of *gypsum* in investigated samples as a predominant phase in all samples is attributed essentially to deterioration processes through solubility of its component surface disintegration, as argued with Chapman and Smith-McNally [45]. The presence of dolomite may be attributed to its being added as a filler to increase strength and stability indexes of stucco. In some specific cases, especially in humid environments, the occurring dolomite may lead to an expansive process, reducing the material's durability through the decomposition of $CaMg(CO_3)_2$ to MgO and CaO that is owed to the effect of temperature [46]. Furthermore, the *decorative elements* consist mainly of calcite and gypsum as major minerals and a high ratio of dolomite, in addition to small amounts of quartz. In this regard, the Turco Master explained the advantages of mixing lime and gypsum mortars, saying, "*The lower proportion of gypsum in relation to lime enables the increase of the speed of the hardening and assures the higher adherence of the mortar, thus compensating for the lower adherence of lime*" [47]. In addition, referring to these materials as covering plasters, he adds, "When *these two materials are used in the making of ornamental or decorative products, the proportion between gypsum and lime varies*" [48]. The higher the lime, the greater the workability, the less the bleed water, the lower the ultimate strength, and the carrying capacity for sand. The lower the sand, the greater the strength. The lower the sand, the greater the workability. The coarser the sand, the less the workability. and the less the likelihood of cracks [49]. The mineral components of the *joint mortar* samples consist of quartz, gypsum, hematite, magnetite, and calcite, where calcite was added to improve the mechanical properties of mortar. The presence of hematite and magnetite is attributed essentially to the presence of red brick fragments as a filler, as could be mentioned previously by some specialists [50-53]. The presence of gypsum is related to salts, and the presence of anhydrite is the result of the transformation of gypsum ($CaSO_4 \cdot 2H_2O$) by thermal weathering [57], [55]. Also, the detection of gypsum in the painted sample is related to the component used in the preparation layer of painting [56].

SEM investigation, Figure 4a, revealed that the structure and components of historical stucco carvings are characterized by the presence of prismatic needle-shaped crystals, as affirmed by Mis-hmastnehi et al. [57]. These crystals are a common feature in historical stucco that is attributed to the formation of gypsum (calcium sulfate dihydrate, $CaSO_4 \cdot 2H_2O$) [58]. They characterized it after hardening through creating a dense, interlocking microstructure that gives stucco its strength, finest features, and value and prevents shrinkage [59]. These characteristics are considered the main key to stucco's durability, texture, and ability to hold complex shapes. Furthermore, the characteristic lamellate form of the gypsum crystals is evident in all samples, Figure 4b, with the notable presence of both Ca and S as two of the essential elements in the gypsum complex; in addition, other impurities (Cu, Al, Na, Cl, Si & Fe) were frequently present [60]. Further SEM investigation focused on the jointing mortar samples, which indicated the use of lime mortar that was composed of calcite, sand, and red brick crumbs (Fig. 4c). Another SEM investigation of mortar samples confirmed the use of lime mortar, consisting of calcite, sand, and gypsum (Fig. 4d).

Microanalysis of samples using EDX demonstrated that gypsum was the predominant component in these samples. Additionally, varying percentages of Si, Ca, Al, Na, Mg, and K were detected. EDX microanalysis of jointing mortar samples indicated a high concentration of Si, Ca, and C; in addition, other elements such as Al, Cl, Na, S, Mg, Fe, and K were also detected in varying proportions. In this regard, the increased calcium (Ca) content confirmed the presence of calcite, likely added to enhance mechanical properties [32]. Finally, the EDX analytical results of the plaster sample highlighted major ions such as Si, Ca, and C, along with minor elements like Al, Cl, Na, S, Mg, and K (Table 3 and Fig. 5). Regarding the precipitation and growth of halite (NaCl) both on materials' surfaces and in pore systems, it could be affirmed that it is due to the seepage of underground water that is widely observed in the artistic elements of the Alexan Pasha Palace façade [61]. This salt is able, by a process of hydration and dehydration, to promote the disintegration of surfaces by its action on other salts [62]. The pressure of salt crystallization enhances the growth and development of micro- and macro-fractures and consequently leads to granular disintegration [63], scales, spalling, and flaking [64] that prevail inside plaster layers and decrease the overall strength of the materials used, especially in the lower parts of the palace walls. So, a lot of these parts have seriously lost their internal cohesion and resistance, where a big percentage of them become powder that was previously corroborated by XRD analysis [65], [66], [67].

FTIR allows classifying the samples as calcite or as mixed mortars (carbonate or carbonate-sulfate) according to the resulting bands, Figure 6. The stretching vibrations of calcium carbonate (1623.77 cm^{-1}, 1622.8 cm^{-1}, 602.646 cm^{-1}, 709.676 cm^{-1}, 874.56 cm^{-1}, 1629.55 cm^{-1}, 876.488 cm^{-1}, 783.922 cm^{-1}, and 875.524 cm^{-1}) were identified in all analyzed samples. Where the vibration frequencies of sulfate are 670 cm^{-1}, 3413.39 cm^{-1}, 3545.49 cm^{-1}, and 3407.6 cm^{-1}. These bands correspond to stretching frequencies of O-H bonds (3547.41 cm^{-1}, 3548.38 cm^{-1}, 3406.64 cm^{-1}, and 3407.6 cm^{-1}) and a bond at 1467.56 cm^{-1} are indicative of the presence of calcium sulfate in samples, while quartz exhibits a stretching vibration bond at 1040.41 cm^{-1} [48], [68]. TGA/DTA analyses proved to be very useful for this purpose. Decomposition of components at specific temperature intervals and the hydraulicity ratio can give important hints on the mortar's character. The integrated thermal analyses (DTA/TGA/DTG) in Fig. 7 (curves A–H) for the 4 samples reveal a technologically and compositionally diverse stucco system comprising gypsum-rich, mixed gypsum–lime, and carbonate-dominated formulations, each reflecting distinct functional roles and preservation states within the architectural stratigraphy. Across all samples, variations in peak sharpness, dehydration temperatures, and mass-loss ratios reflect differences in crystallinity, grain size, and degrees of weathering [69]. The simultaneous presence of gypsum and calcite, as confirmed by XRD, further suggests an intentional choice of materials that combines the fast-setting properties of gypsum [70] with the mechanical strength provided by lime [71].

These compositional differences also may correspond to the functional role of each material [72]: in stucco layers, gypsum appears as the dominant binder used for decorative and finishing purposes, with only minor lime impurities, whereas in the jointing mortar, lime constitutes the main structural component, with small amounts of gypsum either present as a byproduct or intentionally added to accelerate setting. In this regard, by preparing and characterizing selected samples, this work attempted to build a matrix that can be used for the identification of old mortars and that also facilitates the selection of suitable and compatible repair ones for conservation. In our case, it could be affirmed that our case study suffers from aggressive deterioration factors, mechanisms, and related symptoms that are attributed essentially to alternative cycles between air temperature (**AT**) and moisture content (**MC**). From a specialized point of view, increasing the MC is mostly accompanied by decreasing AT in the ambient environment; gypsum becomes more plastic, which leads to further compromising its structural integrity, as attested by Reynaud et al. [73]. While water-induced degradation is often attributed to the index of gypsum's solubility [74], in addition to the effects of other factors such as the material's intrinsic properties, salt content [75], air pollution, and wind-drying effects [76] that also play crucial roles in its degradation and micro-structure features of the gypsum decorative elements. In contrast, the minimal moisture increasing the AT and decreasing the MC can significantly weaken the crystal bonds within gypsum, leading to a reduction in mechanical strength [77], particularly with the presence of other factors. These processes will be studied in further work.

Conclusion

This work aims to examine and analyze the materials used in the façades of Alexan Pasha Palace to identify their components and their deterioration effects and define the salt types, particularly sulfates and halite, which are among the leading causes of deterioration and the detachment of its components, thereby losing its historical authenticity. Then, introduce a scientific study helping in their restoration. Through varying analytical methods, gypsum and calcite were identified as the main decoration component. The analysis showed that the samples consisted of SiO_2, $CaSO_4{\cdot}2H_2O$, and $CaCO_3$; the plaster mortar components were $CaSO_4{\cdot}2H_2O$, $CaCO_3$, and SiO_2. Jointing mortar components included $CaCO_3$, SiO_2, $CaMg(CO_3)_2$, Fe_2O_3, and Fe_3O_4. Furthermore, gypsum was identified as the main component in the decorative elements. Quartz was detected in all samples, in addition to calcite, which was added to improve mechanical properties of the raw materials. Finally, these results will be used in the conservation-restoration interventions of these decoration elements that contribute to the continuity of the artistic and aesthetic value of the archaeological building or decorative element.

References

[1] A. Farghaly, "*Palaces of the city of Assiut during the thirteenth century and the first half of the fourteenth century AH to the nineteenth century and the first half of the twentieth century AD—a comparative archaeological and artistic study*" (MA Dissertation, Archaeology Dep., Faculty of Arts, Assiut Univ., Egypt, p. 43, 2017). (In Arabic).

[2] Sh. Mohammed, "Rehabilitation and reuse of the archaeological palaces in Minia Governorate," *Int. J. of Heritage, Tourism and Hospitality*, vol. 14, no. 1, pp. 276-295, 2020, DOI: 10.21608/ ijhth.2020.128075.

[3] M. El-Gohary, "Investigations on limestone weathering of El-Tuba minaret, El Mehalla, Egypt: A case study," *MAA*, vol. 10, no. 1, pp. 61-79, 2010.

[4] M. Kühlenthal and H. Fischer, "Guidelines and procedures for the restoration of the monuments in Petra," in *Petra, Arbeit Shefte des Bayerischen Landesamtes für Denkmalpflege*, München: ICOMOS, 2000, pp. 84-86.

[5] F. Peña, Á. Díaz, F. Orjales, and J. Pita, "An UAV system for visual inspection and wall thickness measurements in ship surveys," *Measurement*, vol. 238, 2024, DOI: 10.1016/j.measurement.2024.115262.

[6] A. David, N. Linford, and P. Linford, "*Geophysical survey in archaeological field evaluation,*" 2nd ed., English Heritage, 59 p., 2008.

[7] E. Banning, A. Hawkins, and S. Stewart, "Quality assurance in archaeological survey," *J. of Archaeological Method and Theory*, vol. 24, pp. 466-488, 2017, DOI: 10.1007/s10816-016-9274-2.

[8] M. El-Gohary, "Methodological evaluation of some consolidants' interference with ancient Egyptian sandstone 'Edfu Mammisi' as a case study." *Progress in Organic Coatings*, vol. 80, pp. 87-97, 2015, DOI: 10.1016/j. porgcoat.2014.11.021.

[9] P. Pesaresi and C. Rizzi, "New and existing forms of shelter at Herculaneum: improving approaches to facilitate the continuous care of site", *Conservation and Management of Archaeological Sites*, vol. 8, no. 4, pp. 237-252, 2007, DOI: 10.1179/175355208X320784

[10] A. Kamel, H. Marie, and H. Afifi, "Technical examination and restoration of the stucco decorations of El Hasawaty mihrāb, Fatimid period, Cairo, Egypt," *IJCS*, vol. 5, no. 4, pp. 469-478, 2014.

[11] M. El-Gohary and A. Metawa, "Cleaning of architectural bricks using RF plasma: Metallic stains," *IJCS*, vol. 7, no. 3, pp. 669-682, 2016.

[12] M. Ali, M. Alenbaawy, and A. Moussa, "Characteristics of building materials exposed to geoenvironmental impacts in Makaad Radwan, Ottoman Cairo, Egypt," *EJARS*, vol. 1, no. 2, pp. 41-51, 2011.

[13] I. Nicu, "Natural hazards - A threat for immovable cultural heritage. A review," *IJCS*, vol. 8, no. 3, pp. 375-388, 2017.

[14] K. Walsh, J. Berger, and C. Roberts, et al., "Holocene demographic fluctuations, climate and erosion in the Mediterranean: A meta data-analysis", *The Holocene*, vol. 29, no. 5, pp. 864-885, 2019, DOI: 10.1177/09596836198266.

[15] M. El-Gohary and A. Abdel Moneim, "The environmental factors affecting the archaeological buildings in Egypt, 'II Deterioration by severe human activities." *Periodico di Mineralogia*, vol. 90, pp. 261-275, 2021, DOI: 10.13133/2239-1002/17383.

[16] M. El-Gohary, "Behavior of treated and un-treated lime mortar before and after artificial weathering", *Restoration of Buildings & Monuments*, no. 6, pp. 369-380, 2012, DOI: 10.1515/ rbm-2012-6552.

[17] M. Rodriguez-Juarez, E. Perez-Diaz, and G. Lopez-Dominguez, et al., "Development and characterization of lime-based stucco for modern construction and restoration applications based on ancient stuccoes from the 'El Cerrito' pyramid, Querétaro, Mexico," *Case Studies in Construction Materials*, vol. 16, 2022, DOI: 10.1016/j.cscm. 2022.e00875.

[18] H. Marey, A. Kamel, and M. Ali, "Developing low-cost eco-friendly restoration mortars for historic lime-based stucco and building materials," *Periodica Polytechnica Civil Engineering*, vol. 68, no. 2, pp. 657-668, 2024, DOI: 10.3311/PPci.23440.

[19] M. Caroselli, S. Ruffolo, and F. Piqué, "Mortars and plasters—how to manage mortars and plasters conservation", *Archaeological and Anthropological Sciences*, vol. 13, 2021, DOI: 10.1007/s12520-021-01409-x.

[20] A. Kamel, M. El Ghanam, and M. Khedr, "Analytical characterization of some historic stucco busts from Muhammad Ali Family, Egypt," *Acta Physica Polonica A*, vol. 135, no. 3, 2019, DOI: 10.12693/APhysPolA.135.353

[21] A. Kamel, "*Evaluation of sulphate activators as alternative consolidants and the used evaluation methods of fragile stucco monuments consolidants - applied on one of the selected objectives*," Ph.D. dissertation, Faculty of Archaeology, Cairo Univ., Egypt, 2014.

[22] A. Kamel, "Reconstructing the historic stucco mortars using XRD analysis and the calculation of the molecular weights of compounds," *J. of Faculty of Archaeology, SVU*, vol. 12, no. 1, pp. 1-16, 2019, DOI: 10.21608/mkaq. 2019.158575.

[23] A. Scala, F. Gabbrielli, M. Giamello, and S. Mugnaini, "Archaeometric analysis of building mortars used in the historic center of Siena (Italy) between the 13th and 16th centuries," *J. of Archaeological Science: Reports*, vol. 35, 2021 DOI:10.1016/j.jasrep.2021.102790.

[24] M. El-Gohary, "The environmental factors affecting the archaeological buildings in Egypt III: Deterioration by severe seismic hazards'," *EJARS*, vol. 11, no. 2, pp. 147-164, 2021, DOI: 10.21608/ejars.2021.210366.

[25] L. Binda, A. Saisi, and C. Tiraboschi, "Investigation procedures for the diagnosis of historic masonries," *Construction and Building Materials*, vol. 14, no. 4, pp. 199-233, 2000, DOI: 10.1016/S0950-0618(00)00018-0.

[26] A. Osman, W. Bartz, and J. Kosciuk, "Characterization of binding lime mortar used in the ruins of Anba Bishoi Monastery near Sohag (Egypt)," in *Proc. of the 9th Int. Masonry Conf.*, Portugal, University of Minho, Guimarães, 2014, pp. 1-12

[27] J. Elsen, "Microscopy of historic mortars—a review," *Cement and Concrete Research*, vol. 36, no. 8, pp. 1416-1424, 2006, DOI: 10.1016/j.cemconres.2005.12.006.

[28] A. Leslie and M. Eden, *A code of practice for the petrographic examination of mortars, plasters, renders and related materials*, Applied Petrography Group, London, 2008, 24 p., http://www.appliedpetrographygroup.com/ reports.htm

[29] M. Caroselli, J. Válek, J. Zapletalová, A. Felici, D. Frankeová, P. Kozlovcev, G. Nicoli, G. Jean, "Study of materials and technique of late baroque stucco decorations: Baldassarre fontana from Ticino to Czechia," *Heritage*, vol. 4, pp. 1737-1753, 2021, DOI: 10.3390/heritage4030097

[30] N. Bader and W. Al-Gharib, "Restoration and preservation of engraved limestone blocks discovered in Abu Mousa excavation, Suez – Egypt," *IJCS*, vol. 4, no. 1, pp. 25-42, 2013.

[31] M. El-Gohary, "The contrivance of new mud bricks for restoring and preserving the Edfa ancient granary—Sohag, Egypt," *IJCS*, vol. 3, no. 2, pp. 67-78, 2012.

[32] K. Traoré, T. Kabré, and P. Blanchart, "Gehlenite and anorthite crystallization from kaolinite and calcite mix," *Ceramics Int.*, vol. 29, pp. 377-383, 2003.

[33] M. Derrick, D. Stulik, and J. Landry, "*Infrared Spectroscopy in Conservation Science,"* USA, Getty Pub., 252 p., 2000.

[34] A. Duran, L. Perez-Maqueda, J. Poyato, et al., "A thermal study approach to Roman-age wall painting mortars," *J. Thermal Analysis Calorimetry*, vol. 99, no. 803-809, 2010, DOI: 10.1007/ s10973-009-0667-2.

[35] J. Alvarez, C. Montoya, I. Navarro, et al., "Study of the lime renderings decay from Plaza de la Corredera, Cordoba," in *9th Int. Cong. on Deterioration and Conservation of Stone*, vol. 2, Amsterdam, Elsevier, 2000, pp. 873-880.

[36] A. Osman, W. Bartz, and J. Kosciuk, "Characterization of historical mortar used in loom factory site at Abydos," *EJARS*, vol. 6, no. 2, 97-107, 2016, DOI: 10.21608/ejars.2019.23629.

[37] M. El-Gohary, "Environmental impacts: Weathering factors, mechanism, and forms affected the stone decaying in Petra," *J. of African Earth Sciences*, vol. 135, pp. 204-212, 2017, DOI: 10.1016/j.jafrearsci.2017.08.020.

[38] Sh. Omar and A. Kamel, "Archaeometric Study of masonry red bricks and pottery water pipes from the tanks of a Coptic water wheel, Sheikh Hamad, Athribis, Sohag, Egypt," *Advanced Research in Conservation Science*, vol. 4, no. 1, pp. 18-32, 2023, DOI: 10.21608/arcs.2023. 172279.1032.

[39] M. El-Gohary and M. Al-Naddaf, "Characterization of bricks used in the external casing of Roman bath walls 'Gadara-Jordan,'" *MAA*, vol. 9, no. 2, pp. 29-46, 2009.

[40] M. Uccelli, M. Caroselli, and J. Válek, "Characterization of the stucco decoration by Baldassarre fontana in the gallery of the Angels at Uherčice Castle," *J. of Archaeological Science: Reports*, vol. 44, 2022, DOI: 10.1016/ j.jasrep.2022.103493.

[41] U. Nurnburger, "Corrosion of metals in contact with mineral building materials" in *Corrosion of reinforcement in concrete: Monitoring, Inhibitors and Rehabilitation Techniques*, New Delhi, Woodhead Pub. Ltd., 2007, pp. 1-9, DOI: 10.1533/9781845692285.1

[42] S. Ibrahim, H. Refai, D. Kandil, and G. Fackler, "Converting Said Halim Palace into a Museum of Egyptian Education," *EJARS*, vol. 13, no. 2, pp. 331-342, 2023, DOI: 10.21608/ejars. 2023.330916.

[43] D. Rossi, "Jens Kröger, "Sasanian Stucco"", *Abstracta Iranica*, vol. 42-43, 2021, URL: http:// journals.openedition. org/abstractairanica/52608 (2/8/2025).

[44] W. Bartz, J. Kierczaka, M. Gąsior, et al. "Analytical overview of different Baroque plastering techniques applied in the post-Cistercian abbey in Lubiąż (South-Western Poland)," *J. of Cultural Heritage*, vol. 28, pp. 37-47, 2017, DOI: 10.1016/j.culher.2017.07.002.

[45] J. Chapman and R. Smith-McNally, "Storing and handling plaster objects," *Conserve O Gram*, vol. 8, no. 2, 1997. https://www.nps.gov/subjects/museums/upload/08-02_508.pdf. (12/2/2025).

[46] L. Lomakina, I. Garanykov, and P. Fedorov, "Practices of dolomite application in the production of construction materials," *ARPN J. of Engineering and Applied Sciences*, vol. 13, no. 10, pp. 3458-3463, 2018.

[47] E. Salavessa, S. Jalali, L. Sousa, L. Fernandes, and A.-M. Duarte, "Historical plasterwork techniques inspire new formulations," *Construction and Building Materials*, vol. 48, pp. 858-867, 2013, DOI: 10.1016/j.conbuildmat.2013. 07.064

[48] C. Genestar and C. Pons, "Ancient covering plaster mortars from several convents and Islamic and Gothic palaces in Palma de Mallorca (Spain). Analytical characterisation", *J. of Cultural Heritage*, vol. 4, no. 4 pp. 291-298, 2003, DOI: 10.1016/j.culher.2003.02.001

[49] H. Nordmeyer, *Stucco Handbook for Builders*, South River Front Parkway, USA, 29 p., 2001.

[50] H. Ghorab, J. Ragai, and A. Antar, "Surface and bulk properties of ancient Egyptian mortars. Part I: X-ray diffraction studies," *Cement and Concrete Research*, vol. 16, no. 6, pp. 813-822, 1986, DOI: 10.1016/0008-8846(86) 90004-9.

[51] J. Ragai, "Surface and bulk properties of ancient Egyptian mortars. Part III: X-ray diffraction studies (b)," *Cement and Concrete Research*, vol. 18, no. 1, pp. 9-17, 1988, DOI: 10.1016/ 0008-8846(88)90116-0.

[52] J. Ragai, H. Ghorab, and A. Antar, "Surface and bulk properties of ancient Egyptian mortars, part II: Adsorption and infrared studies," *Cement and Concrete Research*, vol. 17, no. 1, pp. 12-21, 1987, DOI: 10.1016/0008-8846(87) 90053-6

[53] S. Sanchez-Moral, J. Martínez, and D. Benavente, "Mechanical Characterisation of ancient Egyptian Mortars," *Key Engineering Materials*, vol. 465, pp. 487-490, 2011, DOI: 10.4028/ www.scientific.net/KEM.465.487.

[54] J. Ragai, "Surface and bulk properties of ancient Egyptian mortars, Part IV: Thermal studies," *Cement and Concrete Research*, vol. 18, no. 2, pp. 179-184, 1988, DOI: 10.1016/ 0008-8846 (88)90002-6.

[55] J. Ragai, "Surface and bulk properties of ancient Egyptian mortars, Part v: Thermal studies (b)," *Cement and Concrete Research*, vol. 19, no. 1, pp. 42-46, 1988. DOI: 10.1016/0008-8846(89)90063-X.

[56] Geology.com. "Barite Mineral." *https://geology.com/minerals/barite.shtml.* (10/5/2025)

[57] M. Mishmastnehi, A. Van Driessche, and G. Smales, et al., "Advanced materials engineering in historical gypsum plaster formulations", *Proceedings of the National Academy of Sciences (PNAS)*, vol. 120, no. 7, 2023, DOI: 10.1073/pnas.2208836120.

[58] M. Philokyprou, "Clay and gypsum mortars used during antiquity in Cyprus," in *Proc. of the 5th Historic Mortars Conf.*, Paris: RILEM, 2019, pp. 226-236.

[59] Aakriti, S. Maiti, and N. Jain, et al., "Synthesis of calcium sulfate whiskers via acidification exploiting FGD gypsum for improved binder properties," *Sustainable Chemistry and Pharmacy*, vol. 42, 2024, DOI: 10.1016/j.scp. 2024.101745.

[60] A. Makled, "*Completion of stuccoes in archaeological buildings: a study of the integrative role between the scientific examinations and analyses and the implementation methods—with an application on a selected stucco object,*" MA dissertation, Conservation Dept., Faculty of Archaeology, Sohag Univ., Egypt, 2025.

[61] J. Lanas, R. Sirera, and J. I. Alvarez, "Study of the mechanical behavior of masonry repair lime-based mortars cured and exposed under different conditions", *Cement and Concrete Research*, vol. 36, pp. 961-970, 2006, DOI: 10.1016/j.cemconres.2005.12.003

[62] M. El-Gohary, “Chemical deterioration of Egyptian limestone affected by saline water,” *IJCS*, vol. 2, no. 1, pp. 17-28, 2011.
[63] M. El-Gohary, “Physical deterioration of Egyptian limestone affected by saline water”, *IJCS*, vol. 4, no. 4, pp. 447-458, 2013.
[64] M. El-Gohary, “Investigations on limestone weathering of El-Tuba minaret, El Mehalla, Egypt: A case study,” *MAA*, vol. 10, no. 1, pp. 61-79, 2010.
[65] M. E. El-Morsy, H. Afifi, H. Mahmoud, et al., “An analytical investigation and a mycological study of some architectural stucco monuments in the period of mamluk and ottoman rule of the Islamic era, Egypt,” *SHEDET*, no. 10, pp. 310-331, 2023, DOI: 10.21608/shedet. 2023.291536.
[66] J. Pozo-Antonio and E. Alonso-Villar, “Stone durability of a surfactant-synthesised alkosylane consolidant on granites with different mineralogy and texture”, *EJARS*, vol. 10, no. 2, pp. 153-164, 2020, DOI: 0.21608/ejars.2020. 131817
[67] M. Abd Elghany, H. Fahid, and M. El-Gohary, “Evaluating the use of ammonium oxalates (amox) in the consolidation of limestone in the temple of Ptolemy XII (Aulits) in Athribis, Sohag,” *EJARS*, vol. 15, no. 2, pp. 229-238, 2025, DOI: 10.21608/ejars.2025.471789
[68] J. Alvarez, I. Navarro, and P. García Casado, “Thermal, mineralogical and chemical studies of the mortars used in the Cathedral of Pamplona (Spain)”, *Thermochimica Acta*, vol. 365, pp. 177-187, 2000, DOI: 10.1016/S0040-6031(00)00624-9.
[69] J. Pires and A. Cruz, “Techniques of thermal analysis applied to the study of cultural heritage," *J. of Thermal Analysis and Calorimetry*, vol. 87, no. 2, pp. 411-415, 2007, DOI: 10. 10.1007/s10973-004-6775-0.
[70] D. Rocha, S. Lucas, and P. Faria, "Experimental optimization of air lime–gypsum mortars by fresh and hardened tests,” *Int. J. of Architectural Heritage*, vol. 20, pp. 1-13, 2026. DOI: 10.1080/15583058.2026.2616400
[71] K. Elert, C. Rodriguez-Navarro, E. Pardo, et al., “Lime mortars for the conservation of historic buildings," *Studies in Conservation*, vol. 47, no. 1, pp. 62-75, 2002, DOI: 10.1179/sic. 2002.47.1.62.
[72] A. Osman, and W. Bartz, “Analysis of mortars applied to the remains surrounding the monastery of Apa Shenoute, Sohag, Egypt,” *Advanced Research in Conservation Science*, vol. 5, no. 2, pp. 70-89, 2024, DOI: 10.21608/arcs.2024.338268.1055.
[73] P. Reynaud, M., Saadaoui, S., Meille, et al., “Water effect on internal friction of set plaster," *Materials Science and Engineering: A*, vol. 442, no. 1-2, pp. 500-503, 2006, DOI: 10.1016/j.msea.2006.01.152.
[74] M. La Russa and S. Ruffolo, “Mortars and plasters–how to characterize mortar and plaster degradation”, *Archaeological and Anthropological Sciences*, vol. 13, no. 10, no. 165, 2021, DOI: 10.1007/s12520-021-01398-x
[75] M. Caroselli, S. Ruffolo, and F. Piqué, “Mortars and plasters—how to manage mortars and plasters conservation”, *Archaeological and Anthropological Sciences*, vol. 13, no. 11, no. 188, 2021, DOI: 10.1007/s12520-021-01409-x
[76] R. Van Hees, L. Binda, I. Papayianni, et al. "Characterization and damage analysis of old mortars," *Materials and Structures*, vol. 37, no. 9, pp. 644-648, 2004, DOI: 10.1007/BF02483293.
[77] A. Shekofteh, A. Hasanpour, and M. Habibzadeh, “Archaeometric characterization of submerged Sasanian stucco from Ghaleh Guri, western Iran,” *Archaeometry*, vol. 68, Suppl. 1, pp. S84-S93, 2025, DOI: 10.1111/arcm.70029.

Received: March 27, 2026
Accepted: July 30, 2026